Nighttime sporadic *E* measurements on an oblique path along the midlatitude trough

A. J. Stocker[1] and E. M. Warrington[1]

Received 25 August 2010; revised 7 December 2010; accepted 28 December 2010; published 3 March 2011.

[1] Observations of nighttime sporadic *E* (Es) made within the HF band on a 1400 km path that lies approximately along the midlatitude trough are presented. Although the probability of occurrence of Es (PEs) is generally below that predicted by the ITU-R model, a significant increase in PEs is found when $K_p \geq 6$. The signal parameters (azimuth, elevation, and Doppler spreads) also increase for high values of K_p. This behavior is consistent with the character of the propagation changing from midlatitude to auroral as the polar cap expands and the trough moves equatorward with increasing K_p.

Citation: Stocker, A. J., and E. M. Warrington (2011), Nighttime sporadic *E* measurements on an oblique path along the midlatitude trough, *Radio Sci.*, *46*, RS2002, doi:10.1029/2010RS004507.

1. Introduction

[2] The appearance of sporadic *E* (Es) can have a number of effects on the propagation of radio signals in the HF and VHF bands. For example, in the HF band, sporadic *E* layers of sufficient intensity can prevent the signal reflecting from the *F* region (i.e., "blanketing") thereby shortening the propagation range. At VHF, Es can enable oblique reflection at frequencies up to around 100 MHz, leading to problems with interference from cochannel transmitters located at ranges well beyond the line of sight. The appearance of sporadic *E* at midlatitudes follows some well-defined seasonal and diurnal variations [see *Whitehead*, 1989] with a strong maximum in the probability of occurrence (PEs) in the summer months and a secondary maximum in winter and a peak during the day with a minimum in the hours before sunrise. PEs has also been mapped as a function of latitude and longitude (although the polar latitudes are not covered) [*Smith*, 1978], work that has been incorporated in an International Telecommunication Union Radiocommunication Sector (ITU-R) recommendation [*ITU-R*, 1999]. There is inconclusive evidence whether longer periodicities, such as the sunspot cycle, are present with some studies showing a positive correlation between PEs and sunspot number (particularly at high latitudes), some negative (particularly at midlatitudes) and some no correlation (e.g., see *Bradley* [2003] and *Whitehead* [1989] for reviews of a number of studies). Recent work [*Maksyutin and Sherstyukov*, 2005] has suggested that the dependencies are complex, since the correlation of PEs with sunspot number was dependent on time of day (positive correlation during the day, negative at night) and the Es critical frequency (positive for foEs = 3–4 MHz and negative for 6–7 MHz). *Stocker and Warrington* [2009] compared nighttime PEs observed on obliquely propagating HF radio waves at sunspot maximum and minimum (the sunspot maximum data set is used in the current paper) and found that PEs was greater at sunspot minimum which is consistent with the results of *Maksyutin and Sherstyukov* [2005]. It is also unclear from previous studies what effect geomagnetic activity has on sporadic *E* since both positive and negative correlations of occurrence and intensity with geomagnetic activity have been found. For example, *Whitehead* [1989] reviewed a number of, largely low and midlatitude, studies and concluded, "magnetic activity does not have much influence on sporadic *E*." However, *Maksyutin and Sherstyukov* [2005] found a seasonal dependence of the response of midlatitude Es to geomagnetic disturbances with a strong (~20%) decrease in the critical frequency in summer and winter, and a weak increase in autumn. They attributed the difference in behavior to a change in the ion composition of the sporadic *E* layer with season.

[3] The midlatitude trough is a nighttime region where the electron density is reduced by a factor of 2 or 3, and forms a boundary between the midlatitude and auroral ionospheres. While there are many studies that have investigated sporadic *E* at midlatitudes, there have been, by comparison, few that have focused on the subauroral region (e.g., in the vicinity of the midlatitude trough). *Rodger et al.* [1983] found that sporadic *E* was commonly observed under both poleward and equatorward edges of the trough (slightly more often on the poleward edge) with the type observed being different before and

[1]Department of Engineering, University of Leicester, Leicester, UK.

0048-6604/11/2010RS004507

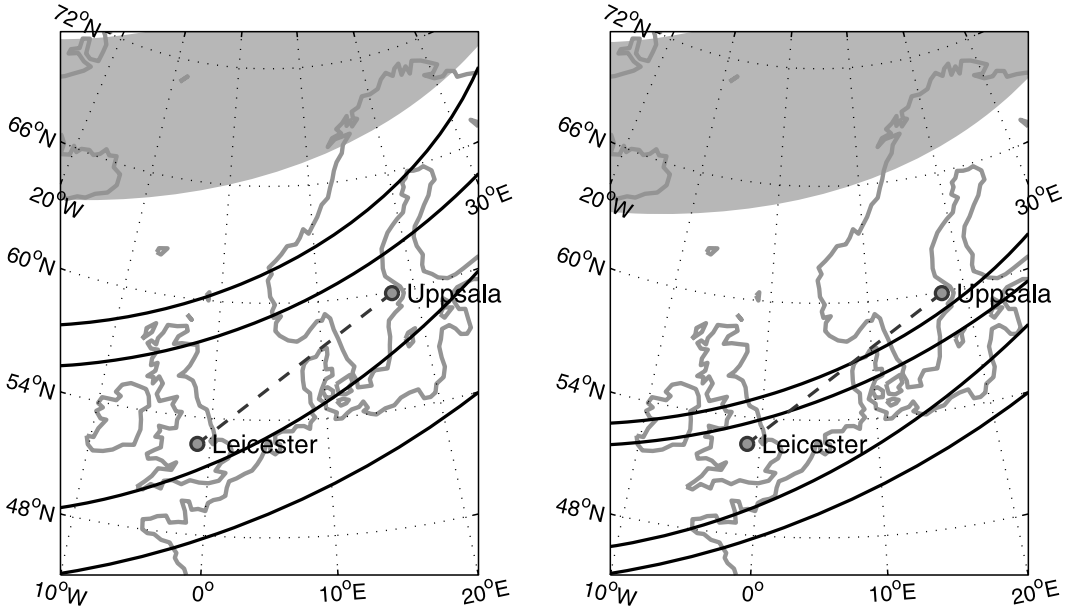

Figure 1. Map illustrating the position of the transmitter and receiver sites in relation to the mid-latitude trough [*Halcrow and Nisbet*, 1977] and auroral oval for (left) $K_p = 4$ and (right) $K_p = 8$. The locations of the trough walls are indicated by the two pairs of lines, while the auroral oval is marked by the shaded region. Note that in Figure 1 (right), the oval is shown for $K_p = 5$ since the model used [*Holzworth and Meng*, 1975] is not valid for higher values.

after magnetic midnight. Retardation, Esr, i.e., where the virtual height of the ionogram trace increases toward the critical frequency, was observed before magnetic midnight, while flat, Esf, i.e., where no increase in virtual height with frequency exists, was observed afterward. *Zherebtsov et al.* [1996] found that in the trough region Esr tended to occur at or just after a minimum in auroral activity (as indicated by the AE index).

[4] While the majority of the studies discussed above have used vertical sounding methods, in this paper observations of the effect of Es on obliquely propagating HF signals are presented. In particular, as well as determining the probability of occurrence of Es, the effects on the characteristics of the reflected HF radio signal, i.e., the distribution of angles of arrival and the spreads in delay, angle of arrival, and Doppler frequency are investigated. Since propagation via Es is common at high and sub-auroral latitudes, an understanding of the HF signal characteristics for these modes is important for those who design and operate systems in these regions (e.g., commercial airlines and shipping).

2. Observations

[5] The experimental arrangement has been described in detail elsewhere [e.g., *Siddle et al.*, 2004] so only a brief overview will be given here. A transmitter located in Uppsala (see Figure 1) radiated a 100 W, Barker coded BPSK signal on six frequencies in the lower HF band (from 4.6 to 18.4 MHz). These signals were received at a site approximately 15 km south of Leicester using a six-channel superresolution DF system. This system was capable of measuring the amplitude and direction of arrival as a function of absolute time of flight (TOF) and Doppler frequency. From these observations, signal parameters such as the delay spread, angular spread, and Doppler spread could then be derived. The system operated from September 2000 until January 2002. An example interval of observations of the TOF and azimuth as a function of time is presented in Figure 2 where propagation modes identified as being via the *E* region are indicated. Unfortunately, propagation from the sporadic *E* and the normal (i.e., solar-controlled) *E* layers cannot be distinguished by these observations, hence the restriction in this paper to nighttime events, when the critical frequency of the normal *E* region will generally be too low to support oblique reflection even at the lowest of the frequencies employed. There are several noteworthy features of the observations presented in Figure 2. First, while propagation via Es occurs on both the nights shown here, no *E* region propagation is observed during the day because *D* region absorption and a low elevation angle (and hence relatively poor antenna performance) lead to the signal at this frequency being too

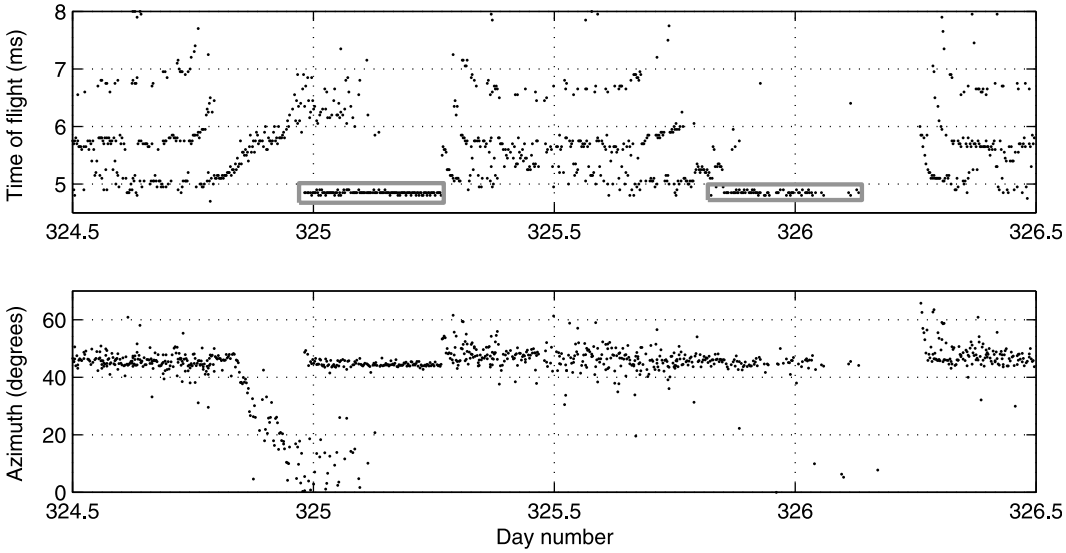

Figure 2. (top) Time of flight (delay) and (bottom) azimuth versus time (UT) for an interval in winter 2001 (20–22 November) for 6.95 MHz. The gray boxes in the Figure 2 (top) indicate the propagation modes identified as being reflected from sporadic *E*.

weak to be detected. Second, at the start of 21 November (day 325) the signal is simultaneously received via both the *F* region and the *E* region. However, the *F* region signal arrives from 30° to 40° north of the great circle direction (46°), while the *E* region signal is received on great circle. This off-great circle propagation, which has been characterized in a number of papers [e.g., *Stocker et al.*, 2009], is predominantly an *F* region effect and is rarely significant for signals reflected from the *E* region. Third, it is apparent that the observed azimuthal variation is greater for signals propagated via the *F* region than it is for those reflected from Es.

2.1. Es Occurrence Statistics

[6] The percentage occurrence of signals identified as having been propagated at night (sunset to sunrise at an altitude of 100 km) via Es layers, together with the ITU predictions [*ITU-R*, 1999], has been plotted as a function of equivalent vertical frequency (foEs) for the different seasons in Figure 3. The oblique frequencies used in the experiment have been converted to the equivalent vertical frequency by dividing them by 5 corresponding to an Es height of approximately 105 km (the exact value depends on the precise height of the Es layer, values vary from 4.7 at 110 km to 5.2 at 100 km). The predicted values have been found by first finding the percentage of time for which foEs > 7 MHz at the midpoint of the Uppsala-Leicester path using the appropriate map given by *ITU-R* [1999]. This value is then used to scale the frequency dependent probabilities for Europe (i.e., region A of *ITU-R* [1999]). The nighttime lines have been determined by applying a correction to the all-day lines (f_{night}/f_{allday}) where f_{night} and f_{allday} are, respectively, the mean nighttime and all-day values of foEs (at 0.1% of the time) derived from the appropriate diurnal variation curves given by *ITU-R* [1999]. While a nighttime line cannot be calculated for the entire year (since there is no diurnal information for this case in the work of *ITU-R* [1999]), the offset from the all-day line must lie between the summer, and winter and equinox extremes. When the observations for the entire year are included in determining PEs, the upper four frequencies (10.4–18.4 MHz) follow the Phillips law (i.e., $\log p = a + bf$, where p is the probability of occurrence of foEs > f, f is frequency in MHz, and a and b are constants) [see *Bradley*, 2003; *ITU-R*, 1999], but are significantly below the value given by the ITU-R model. However, the results for the lowest two frequencies (4.64 and 6.95 MHz) do not follow the Phillips law because of an instrumental effect as follows. At these frequencies, 4.64 MHz in particular, propagation via the *F* region is often observed for a substantial portion of the night. Since the system is capable of resolving only those multiple modes that are separated in TOF by more than approximately 0.5 ms (i.e., the transmitted pulse width) and that have signal strengths within about 15 dB of each other, if the *F* region mode is stronger than *E* region mode by more than this amount, the latter will not be detected. For winter and equinox the behavior is largely similar to that for the entire year, with the upper four frequencies obeying the Phillips rule, although in the case of equinox, PEs derived from the observations is

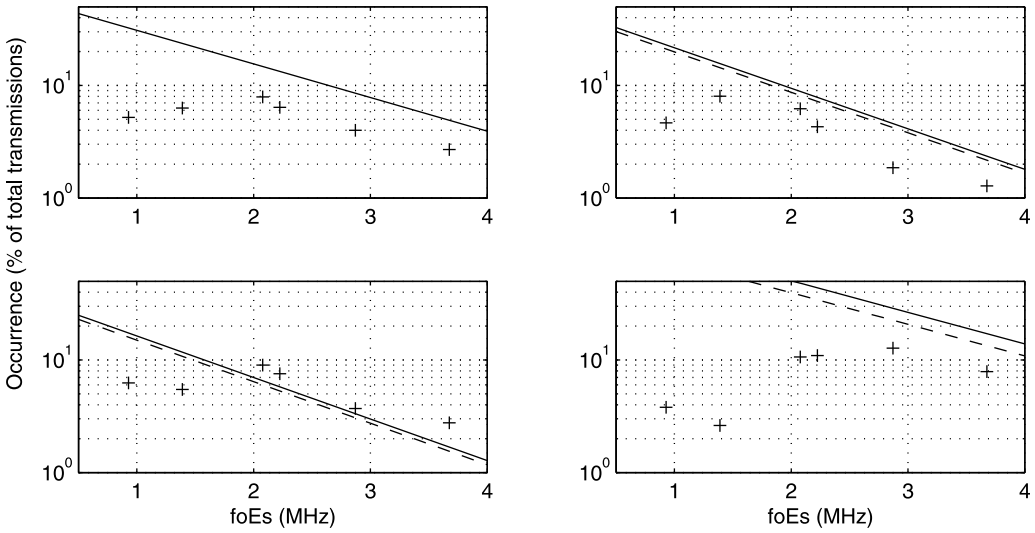

Figure 3. The percentage occurrence of signals propagated via Es in 2001 as a function of equivalent vertical frequency (foEs) for (top left) the entire year (48195 observations), (top right) winter (22630 observations), (bottom left) equinox (19385 observations), and (bottom right) summer (6180 observations). The observations are marked by pluses, while the solid and dashed lines give predictions for the appropriate season from the ITU-R model [*ITU-R*, 1999] for all day and nighttime only, respectively.

slightly higher than that predicted. For the summer, there are fewer observations (because the nighttime interval is substantially reduced) and propagation via the *F* region is more common at all except the highest two frequencies leading to a significant underreporting of the presence of sporadic *E*.

[7] PEs for 2001 is presented as a function of magnetic activity (as represented by the K_p index) in Table 1. From Table 1 it is apparent that the behavior is similar at low (i.e., $K_p < 3$) and moderately disturbed levels of magnetic activity (i.e., $3 \leq K_p < 6$), except for a slightly steeper negative gradient with frequency (for frequencies of 10.39 MHz and higher) in the latter case. Although periods of high levels of magnetic activity (i.e., $K_p \geq 6$) are comparatively rare (just under 3% of the observations), it is clear that that the occurrence of sporadic *E* is significantly more frequent during these intervals (except at 4.64 MHz). This behavior can be explained by the expansion of the polar cap when K_p is high, which in turn leads to the auroral oval and the poleward edge of the trough moving sufficiently far equatorward to lie close to the path midpoint (see Figure 1). Work undertaken in the southern hemisphere [*Rodger et al.*, 1983] also found that Es was slightly more prevalent under the poleward edge of the trough than the equatorward edge.

2.2. Direction of Arrival

[8] The distribution of azimuths at each frequency for all observations of nighttime Es is presented in Figure 4. The peak of the azimuth distribution tends to be centered on the great circle direction (~46°) for all frequencies, while the variation in azimuth tends to decrease with increasing frequency. The two peaks in the distribution that occur for the higher frequencies, the main one, as stated above, close to the great circle direction with a smaller one 2° to the north arise from the resolution in azimuth (2°) employed in generating the steering vectors for the antenna array. This azimuth resolution represents a compromise between precision and computation time (the latter is particularly important since bearings are obtained for each TOF and Doppler in the channel scattering function for which the signal is observed; see section 2.3 of *Warrington et al.* [2000] for more details). Although an interpolation function is used, the resultant bearings tend to cluster around the 2° intervals particularly for the

Table 1. Occurrence of Sporadic *E* (%) for Three Different Levels of Geomagnetic Activity[a]

Frequency (MHz)	$K_p < 3$ (35,304)	$3 \leq K_p < 6$ (11,597)	$6 \leq K_p$ (1,294)
4.64	4.5	7.2	7.4
6.95	5.7	6.8	17.7
10.39	7.2	8.8	18.6
11.12	6.0	6.8	16.0
14.36	4.0	3.0	13.9
18.38	2.7	1.6	14.7

[a]The number of observations obtained in the various ranges of K_p is indicated in the parentheses.

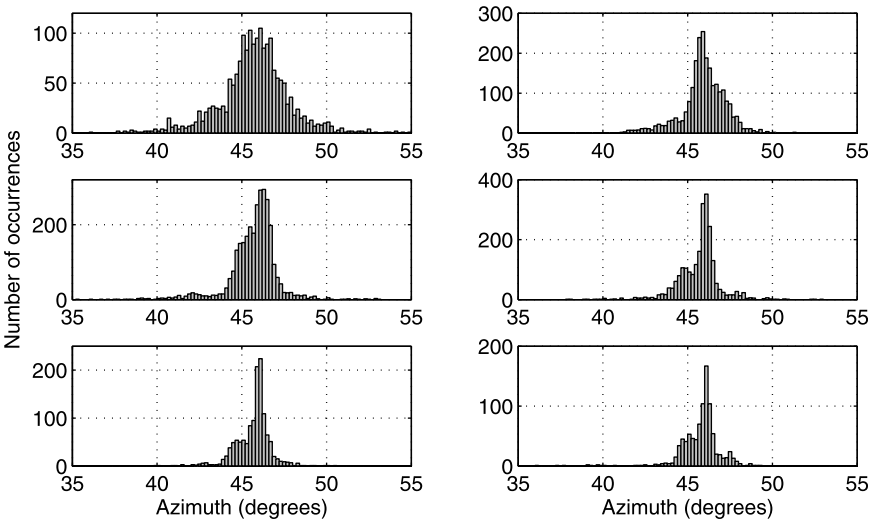

Figure 4. Histograms of the number of occurrences of azimuth of arrival (degrees east of north) for signals propagating via sporadic *E* at frequencies of (top left) 4.64, (top right) 6.95, (middle left) 10.39, (middle right) 11.12, (bottom left) 14.36, and (bottom right) 18.38 MHz.

higher frequencies where the beam width of the antenna array is small. Since the principal aim of the experiment was to study large off great circle effects [e.g., see *Stocker et al.*, 2009] this resolution was usually satisfactory.

[9] The mean azimuth and elevation of arrival for varying levels of K_p are presented in Table 2. For low and medium values of K_p, the azimuth is close to the nominal great circle direction (46°) while at high K_p at frequencies in the range 10.39–14.36 MHz, the azimuth is deviated to the north of the great circle by about 1°. At the same time, for all frequencies except 18.38 MHz, the elevation decreases by about 3°–4° as K_p increases from low to high levels. Although not shown in Table 2, these changes are accompanied by a small increase in mean TOF (less than the resolution of 0.05 ms) at the highest band of K_p. Assuming specular reflection, these small changes in TOF, azimuth, and elevation with increasing K_p are consistent with the location of the reflection point moving away from midpoint toward the transmitter, moving slightly northward of the great circle and the height of the Es layer increasing (see Figure 5). As described in section 2.1, when K_p increases, the polar cap expands and the poleward edge of the trough and auroral oval lie close to the path midpoint, potentially changing the generation mechanism and location and character of the observed Es from midlatitude to auroral.

[10] Although there is a strong seasonal dependence of PEs (see section 2.1), there is no significant systematic effect of season on the directions of arrival, except that the mean elevation for frequencies of 11.12 MHz and less is approximately 2° higher in winter than in summer or at the equinoxes. Since there is no change in the time of flight, assuming specular reflection, this means that the reflection point is closer to the receiver and the reflection height is lower in winter (by approximately 8 km at 10.39 MHz) and there may be a tilt in the Es layer.

2.3. Signal Spreading

[11] An example of the observed channel scattering function, i.e., the signal power, azimuth, and elevation as a function of time delay and Doppler frequency is given in Figure 6. It should be noted that there was a small difference in the frequency references at the transmitter and receiver and this accounts for most of the 2 Hz deviation of the signal from zero Doppler. The signal power as a function of azimuth and elevation for the same observation presented in Figure 6, excluding the signal reflected from the *F* region (i.e., that at a TOF of ~6 ms), is given in Figure 7. In this example, there is some evidence indicating the presence of fine structure within the Es reflection with two peaks in the azimuth distribution separated by 1°–2°. While it is possible that this fine structure results from the angular resolution of the steering vectors (i.e., 2° in azimuth, as explained in section 2.2), previous work [*Sherrill and Smith*, 1977; *Minullin*, 1986] has also found evidence of similar structure. While the range of elevations from which the signal is observed to arrive is considerably larger than that observed by *Clarke and Tibble* [1978], the resolution of the Doppler measurements (0.5 Hz) was insufficient to detect the multiple signal components observed by these authors. Following the methods of *Angling et al.* [1998],

Table 2. Mean and Standard Error of the Mean for Azimuth and Elevation at Three Different Levels of Geomagnetic Activity[a]

Frequency (MHz)	$K_p < 3$ (35,304)	$3 \le K_p < 6$ (11,597)	$6 \le K_p$ (1,294)
	Azimuth (*deg*)		
4.64	45.8 ± 0.1	45.8 ± 0.1	46.1 ± 0.3
6.95	45.75 ± 0.05	45.9 ± 0.1	45.8 ± 0.1
10.39	45.87 ± 0.03	45.73 ± 0.06	44.5 ± 0.2
11.12	45.90 ± 0.04	45.66 ± 0.06	44.6 ± 0.1
14.36	45.73 ± 0.03	45.85 ± 0.06	44.9 ± 0.1
18.38	45.88 ± 0.04	46.0 ± 0.1	45.2 ± 0.2
	Elevation (*deg*)		
4.64	13.8 ± 0.3	11.6 ± 0.3	10.9 ± 1.1
6.95	9.8 ± 0.2	9.5 ± 0.4	7.2 ± 0.6
10.39	9.6 ± 0.2	9.1 ± 0.3	5.6 ± 0.4
11.12	10.5 ± 0.2	9.0 ± 0.3	6.1 ± 0.3
14.36	8.6 ± 0.2	6.8 ± 0.4	5.0 ± 0.3
18.38	7.9 ± 0.2	7.3 ± 0.4	6.6 ± 0.3

[a]The number of observations obtained in the various ranges of K_p is indicated in the parentheses.

Warrington and Stocker [2003], and *Warrington et al.* [2006], the delay, Doppler, azimuth, and elevation spreads (i.e., those containing 80% of the power) were derived for observations of the type presented in Figures 6 and 7. For this particular example, the spreads are 0.02 ms, 1.3 Hz, 4°, and 6°, respectively, putting it into the highest 5% of azimuth spreads observed at 6.95 MHz. The median and 95th percentile values of the spreads found for all Es observations in 2001 have been plotted as a function of frequency in Figure 8. In contrast to the results of *Warrington and Stocker* [2003], the Doppler spread at the 95th percentile increases with increasing frequency, although it should be noted that in the earlier paper reflections from all modes were considered, whereas in the current work only reflections from Es layers are included in the statistics. The delay spread (corrected for the transmitted pulse width) is largely independent of frequency, a result that might be expected since generally sporadic *E* layers are relatively thin. The azimuth and elevation spreads decrease with increasing frequency.

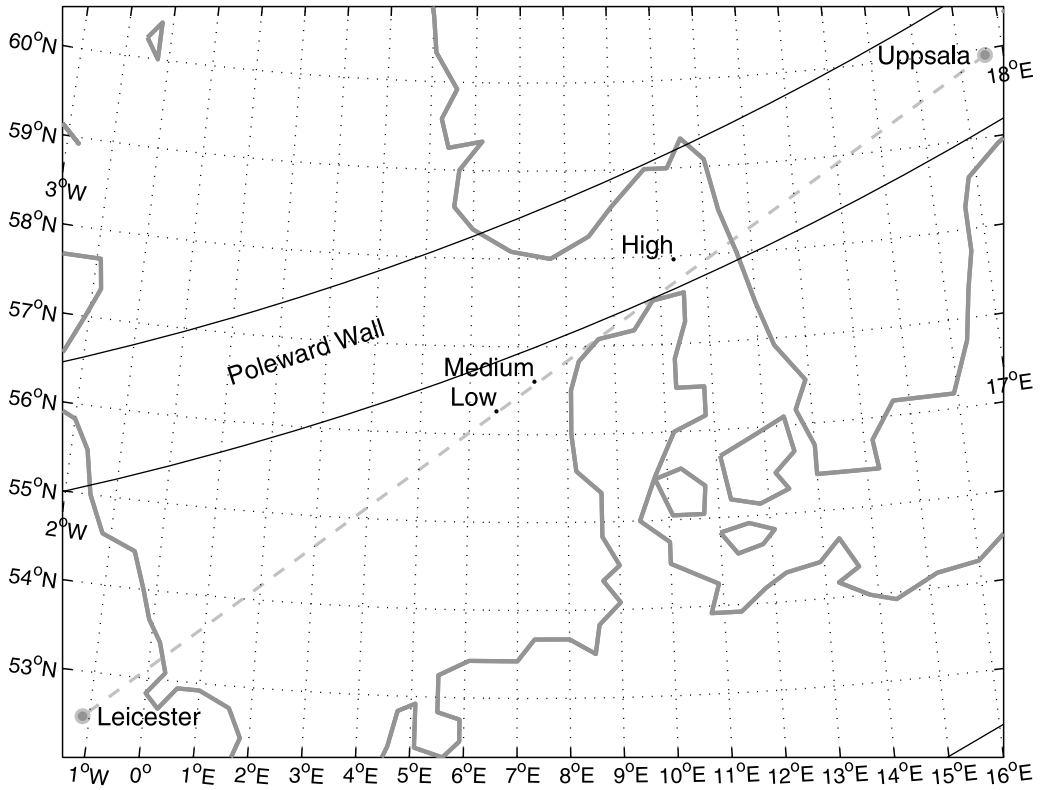

Figure 5. The reflection point of a 10.39 MHz signal at three levels of K_p, low (<3), medium (3–6), and high (>6). The reflection points have been calculated assuming specular reflection using the observed mean values of time of flight, azimuth, and elevation. The modeled position of the poleward wall of the trough on 31 March 2001 at 0000 UT for a value of $K_p = 7-$ is also shown.

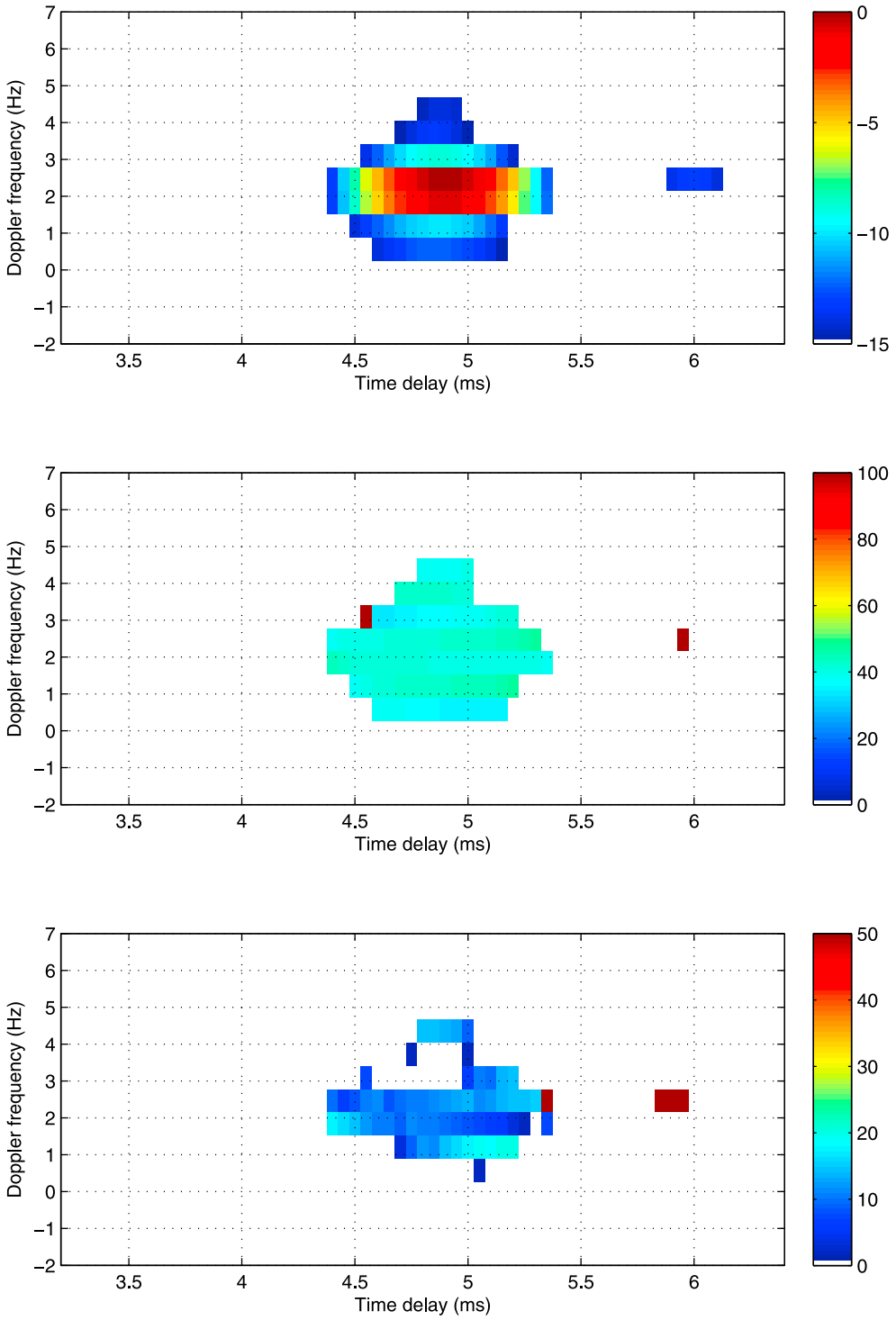

Figure 6. The channel scattering function observed on 16 January 2001 at 2009 UT for a frequency of 6.95 MHz. (top) The signal power (in dB referenced to the peak power), (middle) the azimuth (degrees east of north), and (bottom) the elevation (degrees) have been plotted as a function of Doppler frequency and time delay (i.e., absolute propagation time).

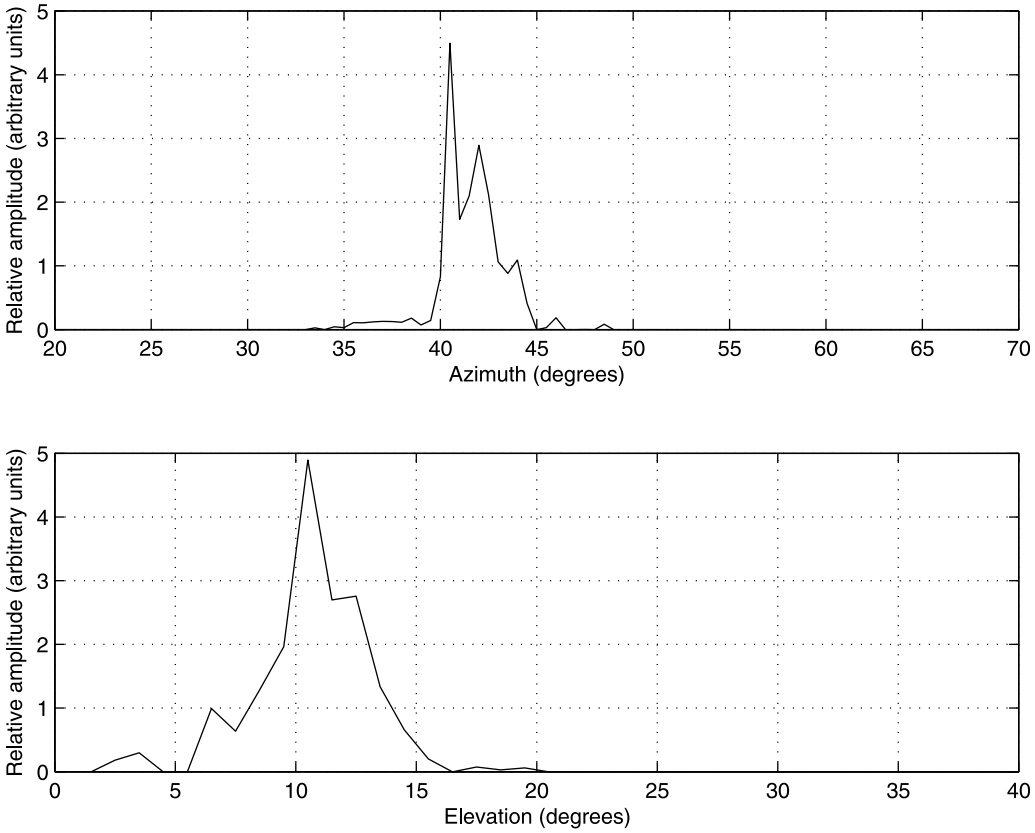

Figure 7. Signal power (in linear units) as a function of (top) azimuth and (bottom) elevation for the same example as Figure 6.

Assuming all the reflections come from the same height, then the median elevation spreads imply that the horizontal dimension of the Es layer is in the range of a few hundred to nearly one thousand kilometers. While these sizes are quite large, they are not entirely inconsistent with previous observations of the horizontal extent of Es at mid and low latitudes [e.g., *Whitehead*, 1989]. However, particularly for the lower frequencies (4.64 and 6.95 MHz) it is possible that both 1-hop and 2-hop Es modes are present (the TOF for these modes are not distinguishable in the observations) and that this then results in the larger elevation spreads.

[12] The mean azimuth, elevation, and Doppler spread as a function of frequency for two different ranges of K_p (low and high) are given in Figure 9 (note delay spread is omitted since it does not change with K_p). As expected, at low K_p the behavior of the mean spreads is similar to that of the median values presented in Figure 8. At high K_p, the spreads are all higher (except elevation spread at 4.64 MHz) than at low K_p, this being particularly marked for the azimuth and Doppler spread at the highest two frequencies. At the high values of K_p the signal is reflected from locations close to or poleward of the trough boundary and therefore propagation is likely to be strongly affected by the presence of irregularities in the trough wall or auroral oval which lead to increases in the azimuth, elevation, and Doppler spreads.

3. Concluding Remarks

[13] Observations of some of the signal parameters of a signal obliquely reflected from sporadic *E*, together with the probability of occurrence of sporadic *E* (PEs), for a year close to sunspot maximum have been presented. The geometry of the path is interesting, since it lies along the midlatitude trough and the character of the propagation changes with geomagnetic activity as the path changes from essentially midlatitude to auroral. The results can be summarized as follows:

[14] 1. With the exception of those obtained during equinox, the values of PEs are generally lower than the ITU-R predictions even when these are adjusted to cover

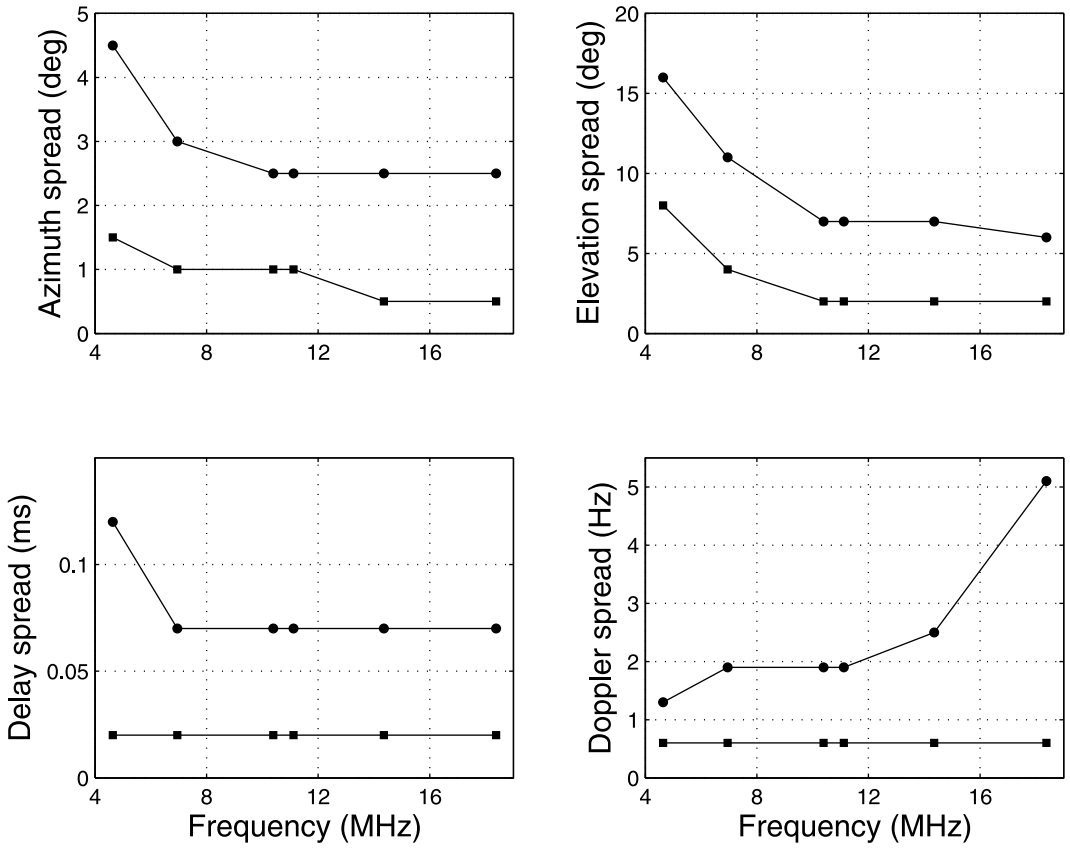

Figure 8. Spread in (top left) azimuth, (top right) elevation, (bottom left) delay, and (bottom right) Doppler versus signal frequency for all Es observations in 2001. The squares represent values of the median, and the circles represent the 95th percentile.

the nighttime only. It is interesting to note that measurements of PEs taken on the same path in 2007 (close to the recent sunspot minimum) have tended to be higher than the predictions [*Stocker and Warrington*, 2009]. However, the relatively small observing intervals (i.e., only 2 years, 2001 and 2007) make it difficult to be certain whether this is a solar cycle effect or part of a longer-term trend (see *Whitehead* [1989] for a discussion of solar cycle effects).

[15] 2. PEs increased significantly during highly disturbed conditions (i.e., when $K_p \geq 6$).

[16] 3. Measurements of the direction of arrival indicate that propagation is largely on great circle, although there is a small deviation (1°) to the north when K_p is very high. The elevation is strongly affected by K_p, decreasing by 3°–4° during very disturbed conditions. Since the TOF remains fixed, this implies an increase of Es height, a northward move in the reflection point and a possible tilt in the Es layer.

[17] 4. The spreads in azimuth, elevation and Doppler all increase during disturbed conditions because of scattering from the irregularities present in the poleward wall of the trough or in the auroral oval. The latter parameter is particularly important for communication systems since, depending on the modulation type employed, it can have a significant effect on the achievable data rate [e.g., *Angling et al.*, 1998]. However, the Doppler spread is significantly lower for the Es layer alone than when all ionospheric modes (i.e., the various *F* region modes) are included [*Warrington and Stocker*, 2003].

[18] From the radio communications perspective, the channel scattering properties of signals reflected via nighttime Es can be significantly better than those reflected by the *F* region (e.g., the delay and Doppler spreads are, in general, reduced). So, operators of HF radio systems on subauroral paths under disturbed magnetic conditions or at high latitudes where the incidence of blanketing Es layers is common [e.g., *Ritchie and*

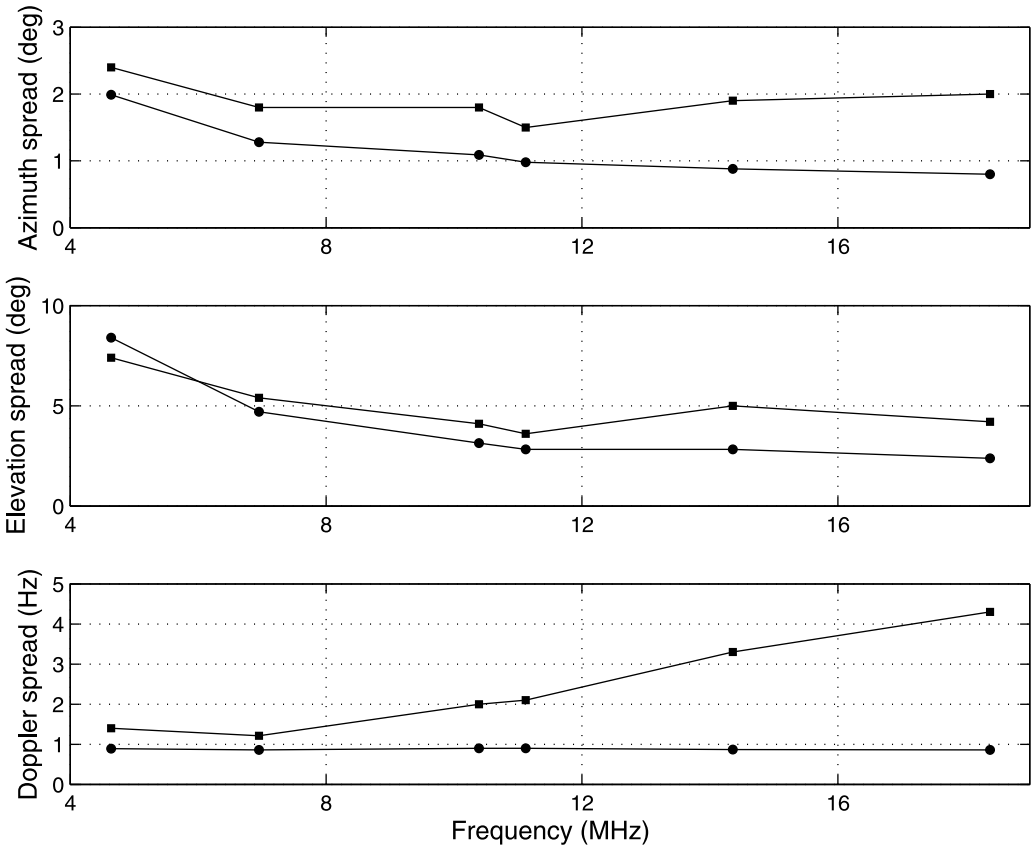

Figure 9. Mean spread in (top) azimuth, (middle) elevation, and (bottom) Doppler versus signal frequency for all Es observations in 2001. The circles represent periods for which $K_p < 6$, while the squares represent intervals when $K_p \geq 6$.

Honary, 2009], might, despite the reduced range, benefit from selecting frequencies or antennas so as to make best use of these conditions.

References

Angling, M. J., P. S. Cannon, N. C. Davies, T. J. Willink, V. Jodalen, and B. Lundborg (1998), Measurements of Doppler and multipath spread on oblique high-latitude HF paths and their use in characterizing data modem performance, *Radio Sci.*, *33*(1), 97–107, doi:10.1029/97RS02206.

Bradley, P. A. (2003), Ingesting a sporadic E model to IRI, *Adv. Space Res.*, *31*, 577–588, doi:10.1016/S0273-1177(03)00053-X.

Clarke, R. H., and D. V. Tibble (1978), Measurement of the elevation angles of arrival of multicomponent h.f skywaves, *Proc. IEE*, *125*, 17–24.

Halcrow, B. W., and J. S. Nisbet (1977), A model of the F_2 peak electron densities in the main trough region of the ionosphere, *Radio Sci.*, *12*, 815–820, doi:10.1029/RS012i005p00815.

Holzworth, R. H., and C.-I. Meng (1975), Mathematical representation of the auroral oval, *Geophys. Res. Lett.*, *2*(9), 377–380, doi:10.1029/GL002i009p00377.

International Telecommunication Union Radiocommunication Sector (ITU-R) (1999), Method for calculating sporadic E field strength, *Recomm. ITU-R P.534–4*, Geneva, Switzerland.

Maksyutin, S. V., and O. N. Sherstyukov (2005), Dependence of E-sporadic layer response on solar and geomagnetic activity variations from its ion composition, *Adv. Space Res.*, *35*, 1496–1499, doi:10.1016/j.asr.2005.05.062.

Minullin, R. G. (1986), The azimuthal arrival angles of radiowaves reflected by the Es layer, *Geomagn. Aeron.*, *26*, 460–463.

Ritchie, S. E., and F. Honary (2009), Observations on the variability and screening effect of Sporadic-E, *J. Atmos. Sol. Terr. Phys.*, *71*(12), 1353–1364, doi:10.1016/j.jastp.2009.05.008.

Rodger, A. S., C. Morrell, and J. R. Dudeney (1983), Studies of sporadic E (Es) associated with the main ionospheric trough, *Radio Sci.*, *18*, 937–946, doi:10.1029/RS018i006p00937.

Sherrill, W. M., and G. A. Smith (1977), Directional dispersion of sporadic E modes between 9 and 14 MHz, *Radio Sci.*, *12*, 773–778, doi:10.1029/RS012i005p00773.

Siddle, D. R., A. J. Stocker, and E. M. Warrington (2004), The time-of-flight and direction of arrival of HF radio signals received over a path along the midlatitude trough: Observations, *Radio Sci.*, *39*, RS4008, doi:10.1029/2004RS003049.

Smith, E. K. (1978), Temperate zone sporadic E maps (f_oE_s > 7 MHz), *Radio Sci.*, *13*, 571–575, doi:10.1029/RS013i003p00571.

Stocker, A. J., and E. M. Warrington (2009), Night-time sporadic E measurements on an oblique path along the mid-latitude trough at sunspot minimum and sunspot maximum, in *Proceedings of IET 11th International Conference on Ionospheric Radio Systems and Techniques (IRST 2009)*, *IET Conf. Publ. 549*, pp. 77–80, Inst. of Eng. and Technol., London.

Stocker, A. J., N. Y. Zaalov, E. M. Warrington, and D. R. Siddle (2009), Observations of HF propagation on a path aligned along the mid-latitude trough, *Adv. Space Res.*, *44*(6), 677–684, doi:10.1016/j.asr.2008.09.038.

Warrington, E. M., and A. J. Stocker (2003), Measurements of the Doppler and multipath spread of HF signals received over a path oriented along the midlatitude trough, *Radio Sci.*, *38*(5), 1080, doi:10.1029/2002RS002815.

Warrington, E. M., C. A. Jackson, and B. Lundborg (2000), The directional diversity of HF signals received over high latitude paths and the possibility of improved data throughput by means of spatial filtering, in *Proceedings of IEE International Conference on Antennas and Propagation (ICAP 2001)*, 17–20 April, pp. 378–382, Inst. of Eng. and Technol., Manchester, U. K.

Warrington, E. M., A. J. Stocker, and D. R. Siddle (2006), Measurement and modelling of HF channel directional spread characteristics for northerly paths, *Radio Sci.*, *41*, RS2006, doi:10.1029/2005RS003294.

Whitehead, J. D. (1989), Recent work on mid-latitude and equatorial sporadic E, *J. Atmos. Terr. Phys.*, *51*, 401–424, doi:10.1016/0021-9169(89)90122-0.

Zherebtsov, G. A., O. M. Pirog, and O. I. Razuvaev (1996), Es-reflections in the region of the main ionospheric trough, *Adv. Space Res.*, *18*, 99–102, doi:10.1016/0273-1177(95)00846-7.

A. J. Stocker and E. M. Warrington, Department of Engineering, University of Leicester, University Road, Leicester LE1 7RH, UK. (emw@leicester.ac.uk)